Engineering synthetic agonists for targeted activation of Notch signaling

David H. Perez[1], Daniel Antfolk[1], Elliot Medina[1], David Gonzalez-Perez[1], Vincent C. Luca[1]

[1] Department of Immunology, Moffitt Cancer Center, Tampa, FL 33602, USA

ABSTRACT

Notch signaling regulates cell fate decisions and has context-dependent tumorigenic or tumor suppressor functions. Although several Notch inhibitors are under development as cancer therapies, the mechanical force requirement for Notch receptor activation has hindered attempts to generate soluble agonists. To address this problem, we engineered synthetic Notch agonist (SNAG) proteins that mimic the tension-generating mechanism of endogenous ligands. SNAGs were designed by fusing a high-affinity variant of the Notch ligand Delta-like 4 (DLL4) to antibody fragments that induce target internalization. This bispecific format enables the SNAG-bound biomarkers to "pull" on Notch receptors, triggering Notch activation in mixed populations of biomarker-expressing and non-expressing cells. SNAGs targeting the immune checkpoint PDL1 potently activated Notch in co-cultures of Notch1- and PDL1-expressing cells, but not in monocultures of Notch1-expressing cells alone. Additional SNAGs targeting the tumor antigens CD19 and HER2 also activated Notch in mixed cell populations, indicating that the SNAG design concept is adaptable to multiple biomarkers. SNAG-mediated Notch activation was blocked by a dynamin inhibitor, and efficacy increased dramatically when SNAGs were dimerized via fusion to antibody Fc domains, suggesting that endocytosis and multimerization are important for optimal SNAG function. These insights will greatly expand our ability to modulate Notch signaling for applications in immunotherapy and regenerative medicine.

INTRODUCTION

The Notch pathway is a conserved signaling system that regulates cell fate decisions, tissue homeostasis, and immune cell development. Notch receptors are massive (~290kD) transmembrane proteins that are activated by a distinctive, mechanical force-driven mechanism[1–4]. Notch signaling is initiated when a Delta-like (DLL) or Jagged (JAG) ligand forms a *trans*-interaction with a Notch receptor on the surface of an adjacent cell[4–7]. Endocytosis of the ligand then generates a "pulling" force that propagates to the negative regulatory region (NRR) of Notch [1,8]. This pulling destabilizes the NRR, which exposes internal cleavage sites for processing by the

intramembrane proteases ADAM10 (S2 cleavage) and γ-secretase (S3 cleavage)[9,10]. Following these proteolytic events, the Notch intracellular domain (NICD) translocates to the nucleus to function as a transcriptional co-activator[11].

Dysfunctional Notch signaling causes numerous inherited and acquired diseases. Loss-of-function mutations in Notch receptors and ligands are linked to the development of aortic valve disease (Notch1), Alagille syndrome (Notch2, Jagged1), CADASIL (Notch3), spondylocostal dysostosis (DLL3), and other congenital disorders[12–15]. In cancer, Notch functions as a tumor suppressor or oncogene depending on the cell type, and both loss-of-function and hyperactivating mutations influence tumorigenesis and disease progression[16]. Notch is also pleiotropic in the context of cell fate decisions, in that Notch activation may stimulate either proliferation or differentiation in different stem cell populations[17]. These diverse functions suggest that Notch agonists and antagonists may each be viable therapeutics in certain biomedical contexts[18].

The role of Notch in T cell biology has led to the development of several Notch-based strategies for enhancing cancer immunotherapy. Notch signaling is important for several natural stages of T cell maturation[19], and ex vivo Notch activation is required for the differentiation of T cells from hematopoietic stem cells (HSCs)[20]. This latter function may potentially be used to generate allogeneic T cells for “off-the-shelf” adoptive T cell or CAR T cell therapies. More recently, Notch activation has been shown to enhance the antitumor function of fully mature, activated T cells[21]. Genetic overexpression of an activated form of Notch[22], as well as culturing T cells in the presence of Notch1-specific antibodies[23] or ligand-expressing cells[24], were each associated with improved tumor clearance in various animal models of cancer. Detailed analysis of the T cells used in these studies revealed that these phenotypes were due to the Notch-stimulated induction of exhaustion-resistant or stem-like phenotypes.

Although Notch inhibitors are widely available, the requirement for mechanical force in Notch activation has precluded the development of soluble agonists[3,18]. Specifically, these agents are challenging to engineer because they must somehow “pull” on the Notch receptor despite lacking a method of force generation. Several strategies have been developed to activate Notch receptors *in vitro* through mimicry of the physiological activation process. Notch signaling may be induced through co-culture of Notch-expressing cells and ligand-expressing cells, by culturing Notch-expressing cells on plates coated with ligands or antibodies, or by administration of ligand-coated

microbeads[23,25,26]. By contrast, only a single antibody targeting Notch3, A13, has been reported to function as a soluble agonist[27]. Binding of this antibody promotes the unfolding of metastable Notch3 NRR domains, which in turn exposes the S2 site for proteolytic cleavage [28]. Unfortunately, this NRR unfolding approach has been ineffective for receptor subtypes with stable NRRs (e.g., Notch1/2/4), and the lack of soluble agonists remains a significant void in our biochemical toolkit for manipulating the Notch pathway.

In this study, we engineered bispecific proteins that stimulate Notch activation in specific cellular contexts. These synthetic Notch agonists (SNAGs) contain a Notch-binding arm and a targeting arm, enabling them to form intercellular interactions in mixed populations of biomarker-expressing and non-expressing cells. A diverse panel of SNAGs stimulated Notch activation via a mechanism that resembles the natural endocytic “pulling” of DLL and JAG ligands, and SNAG efficacy was enhanced through the incorporation of a multimerization scaffold. We validated our SNAG design in a model system by restoring the signaling of loss-of-function DLL4, and we successfully developed additional SNAGs targeting the tumor biomarkers PDL1, CD19, and HER2. The modularity and versatility of this SNAG platform provide a blueprint for the development of a diverse repertoire of Notch-based biologics.

RESULTS

Soluble DLL4 ligand multimers do not activate Notch signaling. As an initial attempt to generate Notch agonists, we investigated whether soluble oligomers of an affinity-matured DLL4 ligand (Delta^{MAX}) activate Notch signaling[29]. Delta^{MAX} contains ten mutations that increase its affinity for human Notch receptors by 500- to 1000-fold, making it a more potent activator than DLL4 in co-culture and plate-bound formats[29]. We hypothesized that this increased affinity, coupled with receptor crosslinking through multimerization, could introduce tension in the absence of an endocytic pulling force. To test this hypothesis, we incubated Notch1-Gal4 mCitrine reporter cells[30] with soluble and immobilized Delta^{MAX} multimers (Fig. 1a-c). Delta^{MAX} dimers were generated through the C-terminal addition of a dimeric human IgG1 Fc domain (Fig. 1b), and tetramers were generated by pre-mixing a 4:1 molar ratio of biotinylated Delta^{MAX} with streptavidin (SA, Fig. 1c). We found that neither the monomers nor the multimers induced reporter activity. By contrast, the plated Delta^{MAX} ligands potently stimulated Notch1 activation (Fig. 1). This indicates that the receptor crosslinking by Delta^{MAX}-Fc dimers and Delta^{MAX}-SA tetramers is insufficient for signaling activation.

Design of synthetic Notch agonists. To develop soluble Notch agonists, we engineered bispecific proteins that recapitulate the endocytosis-linked activation mechanism of DLL and JAG ligands (Fig. 2a). SNAGs were created by fusing Delta^{MAX} to the N-terminus of biomarker-targeting antibody fragments via a flexible $(GS)_5$ linker, or by fusing Delta^{MAX} and antibody fragments to the N- and C-termini of a dimeric IgG1 Fc domain (Fig. 2b). These design concepts are intended to form a "molecular bridge" between Notch-expressing cells and cells that express a given surface protein. Conceptually, SNAGs should then activate Notch if the enforced interactions induce endocytic or tensile force capable of unfolding the NRR.

SNAGs rescue the signaling of a signaling-deficient DLL4 mutant. To demonstrate proof-of-concept, we tested whether a SNAG could rescue the activity of a signaling-deficient DLL4 mutant. Loss-of-function DLL4 cells were generated by expressing a "headless" DLL4 truncation where the Notch-binding C2 and DSL domains[6,31] were replaced with a BC2 epitope tag (BC2-DLL4^{HL}) (Fig. 3a)[32]. BC2-SNAGs were then generated by fusing Delta^{MAX} to a BC2-specific nanobody (Figs. 3a-b). We found that BC2-DLL4^{HL} cells alone did not activate signaling in a Notch1-Gal4 mCitrine reporter assay, whereas the addition of 1 nM to 100 nM concentrations of SNAGs stimulated a dose-dependent increase in reporter activity (Fig. 3c). Monomeric BC2-SNAGs containing the $(GS)_5$ linker (BC2-SNAG) stimulated a ~6-fold increase in Notch1 signaling, whereas dimeric BC2-SNAG Fc fusion proteins (BC2-SNAG^{Fc}) were more effective and induced a ~10-fold increase (Fig. 3c). Importantly, administration of the monomeric or dimeric BC2-SNAGs alone did not substantially increase Notch1 reporter activity, indicating that a mixture of target-expressing and non-expressing cells is required for SNAG-mediated activation (Fig. 3c).

SNAGs targeting tumor antigens activate Notch in mixed cell populations. We next tested whether SNAGs targeting the tumor antigens PDL1, CD19, or HER2 can stimulate Notch activation. There is mounting evidence that Notch signaling enhances the function of activated T cells[22–24], and SNAGs localized to the tumor microenvironment have the potential to stimulate localized activation of tumor-associated lymphocytes. For these SNAGs, the targeting arms were derived from antibody-drug conjugates (ADCs) that were pre-selected for their ability to induce target internalization. We hypothesized that SNAGs incorporating ADC antibodies could thus mimic the physiological endocytosis mechanism of DLL or JAG ligands.

We generated monomeric and dimeric PDL1-SNAGs by fusing Delta^{MAX} to a single-chain variable fragment (scFv) derived from the ADC antibody Atezolizumab[33,34]. In the monomeric PDL1-SNAG, Delta^{MAX} and the scFv were connecting using a $(GS)_5$ linker, and in the dimeric PDL1-SNAG (PDL1-SNAG^{Fc}), Delta^{MAX} and the scFv were fused to the N- and C-termini of an IgG1 Fc domain. Unexpectedly, addition of the monomeric PDL1-SNAG to a 1:1 mixture of Notch1 reporter cells and PDL1-expressing MDA-MB-231 cells did not activate Notch1 (Fig. 4a). However, the dimeric PDL1-SNAG^{Fc} protein stimulated a ~7-fold increase in Notch1 signaling in the coculture, suggesting that multimerization or avidity-enhancement may be required for SNAGs to effectively target biomarkers other than Notch ligands (Fig. 4a). Neither the PDL1-SNAG nor the PDL1-SNAG^{Fc} substantially increased Notch1 reporter activity in the absence of MDA-MB-231 cells. Because of the increased efficacy of the dimeric SNAGs (Fig. 3c, Fig. 4a), we designed subsequent SNAGs using only the Fc-fusion format.

SNAGs do not activate signaling on cells expressing both Notch1 and PDL1. Given the ubiquitous expression of Notch1 in mammalian cells, it is conceivable that SNAGs could activate signaling when Notch1 and the target protein are both present on the cell surface. To test this possibility, we cultured MDA-MB-231 cells in the presence of soluble Delta^{MAX}-Fc, PDL1-SNAG^{Fc}, or immobilized Delta^{MAX}-Fc and monitored the levels activated Notch1 by Western Blot (Fig. 4b). We found that the plated Delta^{MAX}-Fc protein stimulated high levels of Notch1 activation, whereas the PDL1-SNAG-Fc did not induce signaling over the background levels observed for soluble Delta^{MAX}-Fc alone (Fig. 4b). The inability of SNAGs to activate Notch1 in MDA-MB-231 cells suggests that the present design does not enable sufficient intercellular crosslinking in cultures of cells expressing both Notch1 and the biomarker.

Development of SNAGs targeting CD19 and HER2. The optimization of PDL1-SNAGs guided our design of additional SNAGs targeting the B cell lymphoma antigen CD19 and the breast cancer antigen HER2. To generate a CD19-SNAG construct, we fused an scFv derived from the CD19-targeting ADC Loncastuximab[35] to the C-terminus of Delta^{MAX}-Fc (CD19-SNAG^{Fc}). The CD19-SNAG was then added to Notch1 reporter cells or to co-cultures of Notch1 reporter cells and CD19-overexpressing 3T3 fibroblast cells. We found that the CD19-SNAG^{Fc} protein stimulated up to a 6-fold increase in reporter activity in the co-culture compared to untreated Notch1 cells (Fig. 4c). For the HER2-SNAG^{Fc} construct, we used an scFv derived from the HER2-targeting ADC Trastuzumab[36] as the targeting arm. Addition of the HER2-SNAG^{Fc} to a mixed

166 culture of Notch1 reporter cells and HER2-expressing SK-BR-3 breast cancer cells induced a 6-
167 fold increase in reporter activity (Fig. 4d) at the highest concentration tested (100 nM), which is
168 similar to the level of activation we observed for the PDL1-SNAG^{Fc} and the CD19-SNAG^{Fc}
169 constructs (Fig. 4a-c). In the absence of biomarker-expressing cells, neither the CD19-SNAG^{Fc}
170 nor the HER2-SNAG^{Fc} stimulated a significant increase in signaling compared to Delta^{MAX}-Fc
171 alone (Fig. 4). Collectively, these data indicate SNAGs may be adapted to target a wide range of
172 cell surface proteins.
173
174 **Endocytosis is required for SNAG-mediated Notch activation.** Ligand endocytosis is
175 important for Notch activation[37], and this process is regulated by ubiquitination of DLL or JAG
176 ICDs by the E3 ligase Mindbomb1[38–40]. To test whether endocytosis also occurs with a SNAG
177 targeting a cell surface protein that is not derived from a natural Notch ligand, we performed an
178 immunofluorescent endocytosis assay utilizing CD19-SNAG^{Fc} in CD19-expressing cells. CD19-
179 SNAG^{Fc} coupled with anti-Fc 647 bound strongly to the surface of the CD19-expressing cells
180 when the mixture was incubated on ice (Fig 5a). The contours of the cells were identified by
181 staining for filamentous actin. Incubating the cells at 37 °C after attaching CD19-SNAG^{Fc}-647 to
182 cells allowed for cellular functions, including endocytosis, to resume. Visualizing the cells after a
183 15 min incubation at 37 °C showed that the majority of CD19-SNAG^{Fc} is internalized (Fig. 5b).
184
185 To test whether endocytosis is necessary for SNAG function, we co-administered SNAGs with
186 the dynamin-dependent endocytosis inhibitor Dynasore. We found that Dynasore completely
187 ablated the activity of CD19-SNAG^{Fc} in co-cultures of Notch1- and CD19-expressing cells,
188 indicating that endocytosis is required for SNAG-mediated activation utilizing CD19 as a
189 biomarker (Fig. 5c). We further found that BC2-SNAGs targeting BC2-DLL4^{HL} were unable to
190 activate Notch1 in co-cultures of Notch1 and BC2-DLL4^{HL} cells in the presence of Dynasore,
191 confirming that endocytosis is also required for SNAG-mediated rescue of DLL4 signaling (Fig
192 5d-e.) Interestingly, we found that immobilized SNAGs were also unable to activate Notch1 in the
193 presence of Dynasore, suggesting that endocytosis in the Notch-receptor cell is essential for
194 Notch activation by plated ligands (Fig. 5f). These studies demonstrate that Notch activation by
195 plated ligands, SNAGs targeting a DLL4 loss-of-function mutant, and SNAGs targeting tumor
196 antigens each depend on endocytosis. However, it is currently unclear whether endocytosis of
197 the receptor, ligand, or both, is essential for SNAG function.
198

DISCUSSION

The development of soluble agonists has been an enduring challenge in the Notch field[18,42]. The SNAG platform described here provides a potential solution to this problem and provides a framework for the development of a diverse array of Notch activating biologics. Such agents have a wide range of potential translational applications, particularly in cancers where Notch functions as a tumor suppressor[16], T cell manufacturing[20,26], T cell immunotherapy[22–24], wound healing[43], and other areas of regenerative medicine. These first-generation SNAGs were engineered using an Fc-fusion format used in clinically viable protein drugs, which may also help to accelerate *in vivo* translation.

In their present form, SNAGs facilitate potent activation of Notch signaling in mixed populations of cells. However, we anticipate that the design may be tuned to further optimize SNAG function. For example, it may be preferable to engineer SNAGs such that the target binding arm has a higher binding affinity than the Notch-binding arm to improve specificity and tissue distribution. Such strategies have been successfully employed both for bispecific inhibitory antibodies[44] and T cell engagers[45]. Additionally, higher-order oligomers beyond the monomeric and dimeric SNAG scaffolds tested here may lead to increased signaling potency. Future studies will focus on optimizing affinity and multimerization to maximize signaling while maintaining favorable biochemical properties.

One surprising observation was that PDL1-SNAGs did not activate signaling on cells expressing both PDL1 and Notch1. We speculate that these SNAGs engage the two targets in *cis* on the surface of a single cell, as opposed to bridging PDL1 and Notch1 proteins between cells, and that *cis* interactions do not introduce sufficient tension to unfold the NRR. This may be attributed to the restricted diffusion of SNAGs in the 2-dimensional environment of the membrane, which can promote preferential *cis* interactions by increasing the local concentration. Previous studies have shown that *cis* inhibition of Notch signaling occurs when ligands and receptors are expressed on the same cell[30,46], and it appears that SNAGs are similarly unable to activate Notch in this context. Regardless, the ability of SNAGs to mediate unidirectional signaling enables highly selective targeting, which could minimize the risks of potential toxicity from global Notch agonism.

Although SNAGs are effective in mixed cell populations, the development of “unconditional” agonists that do not rely on a secondary target remains an unsolved problem. Thus far, it appears

that the metastable NRR of Notch3 is uniquely susceptible to antibody-mediated destabilization[28,47]. The engineering of agonists targeting other Notch receptors with more stable NRRs may require alternative solutions. The successful activation of Notch1 with ligands immobilized on beads[26] or DNA origami structures[48] suggests that oligomerization may be an effective strategy, but these methods are not currently viable for in vivo applications. Despite these limitations, the development of SNAGs represents a key first step towards the widespread development of Notch activating molecules for basic and translational research.

AUTHOR CONTRIBUTIONS

V.C.L. and D.H.P. wrote the manuscript. V.C.L., D.H.P, and D.A. designed the experiments. D.H.P. cloned the SNAG constructs, purified the proteins, and performed the signaling assays. E.M. and D.G.P. generated the Delta^{MAX} constructs. D.A. performed the Notch activation assays in MDA-MB-231 cells and immunofluorescent endocytosis assays. V.C.L. supervised the project and edited the manuscript.

ACKNOWLEDGEMENTS.

This project was supported by NIH R35GM133482 (V.C.L. and D.A.), the Sigrid Juselius Foundation (D.A.) and NIH R35 Diversity Supplement R35GM133482-03S2 (E.M.). V.C.L. is a Rita Allen Scholar. Shared resources were provided by the Moffitt Cancer Center Support Grant NIH P30CA076292.

COMPETING INTERESTS

V.C.L. is a consultant on unrelated projects for Cellestia Biotech, Remunix, and Curie.Bio. The remaining authors have no competing interests.

FIGURES

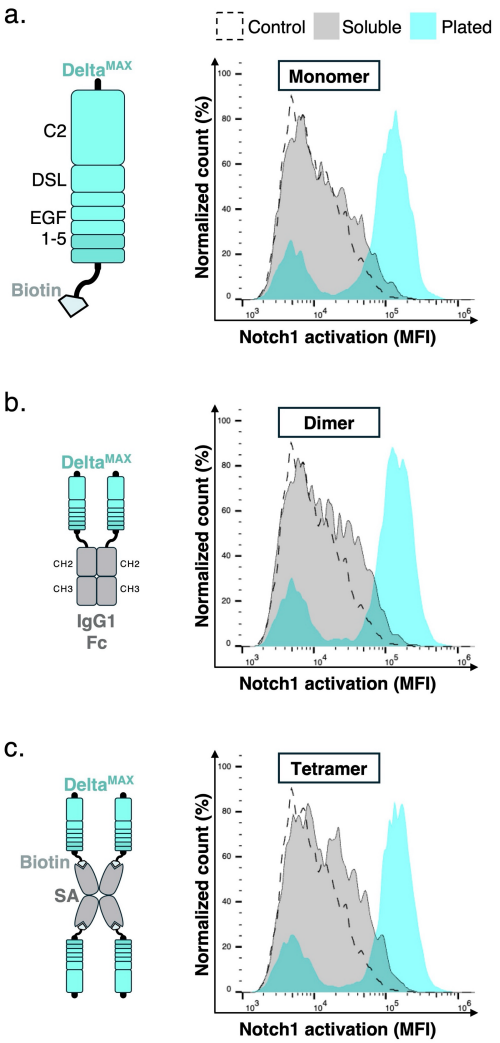

Figure. 1. Soluble Delta^{MAX} oligomers do not activate Notch signaling. (a) Flow cytometry histogram overlay of Notch1 reporter cells stimulated by soluble or plated (non-specifically adsorbed) Delta^{MAX}. The cartoon depicts the site-specifically biotinylated Delta^{MAX}(N-EGF5) construct. (b) Histogram overlay of Notch1 reporter cells stimulated with soluble or plated Delta^{MAX}-Fc protein. (c) Histogram overlay of Notch1 reporter cells stimulated with plated or soluble Delta^{MAX}-SA tetramers.

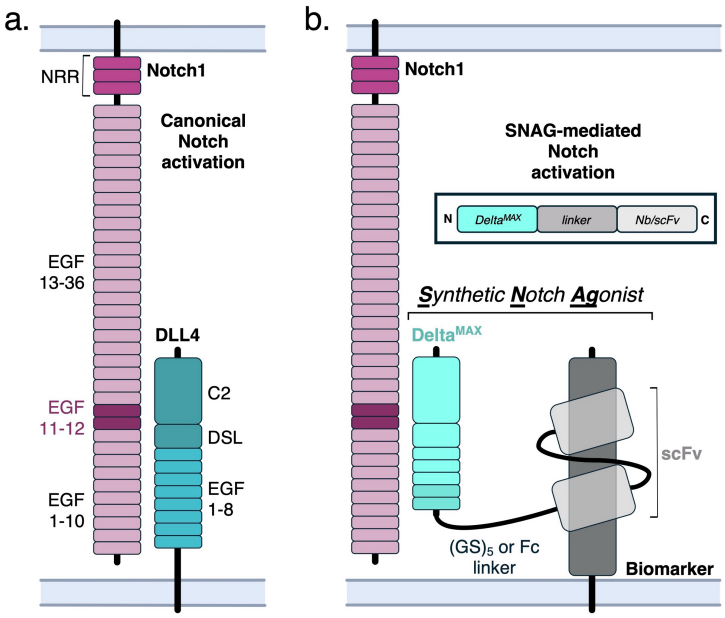

Figure 2. Design concept for synthetic Notch agonists. (a) Cartoon schematic depicting the ECDs of Notch1 and DLL4 interacting during canonical Notch activation. The primary ligand-binding region of Notch1 (EGF domains 11-12) and the primary receptor-binding region of DLL4 (C2 and DSL domains) are shaded. (b) Schematic of a generalized SNAG construct alongside a cartoon depicting SNAG-mediated Notch activation.

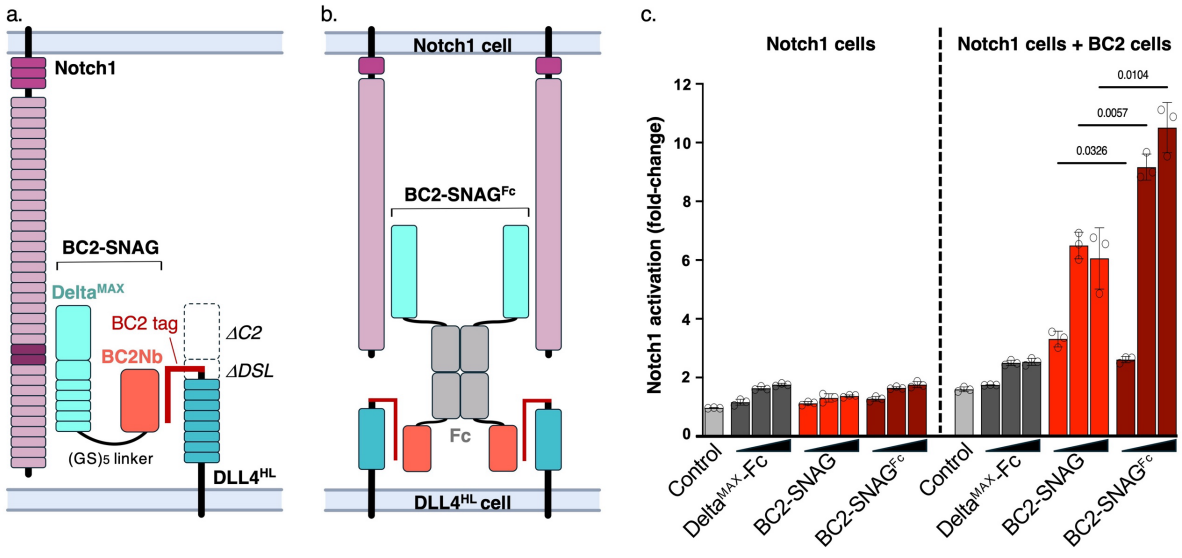

Figure. 3. SNAGs rescue the signaling of a loss-of-function DLL4 mutant. (a) Cartoon schematic depicting a SNAG binding to Notch1 and a loss-of-function DLL4 mutant. The "headless" loss-of-function DLL4 protein ($DLL4^{HL}$) was generated by replacing the Notch-binding C2-DSL region with a BC2 peptide epitope recognized by the anti-BC2 nanobody. (b) Cartoon schematic depicting the multivalent binding of a dimeric Fc-tagged SNAG ($BC2\text{-}SNAG^{Fc}$) to Notch1 and "headless" DLL4. (c) A fluorescent reporter assay was used to evaluate SNAG-mediated activation of Notch1. Increasing concentrations (1 nM, 10 nM, or 100 nM) of $Delta^{MAX}$-Fc, BC2-SNAG, or $BC2\text{-}SNAG^{Fc}$ were added to Notch1-Gal4 mCitrine reporter cells alone or a 1:1 mixture of Notch1 reporter cells and HEK293 cells expressing $DLL4^{HL}$ and fluorescence was measured by flow cytometry. A representative experiment from three biological replicates is shown. Mean fluorescence intensity (MFI) was normalized to the mean MFI of Notch1 reporter cells alone. Error bars represent the standard deviation of three technical replicates with the *P* value by Student's *t* test shown above each comparison.

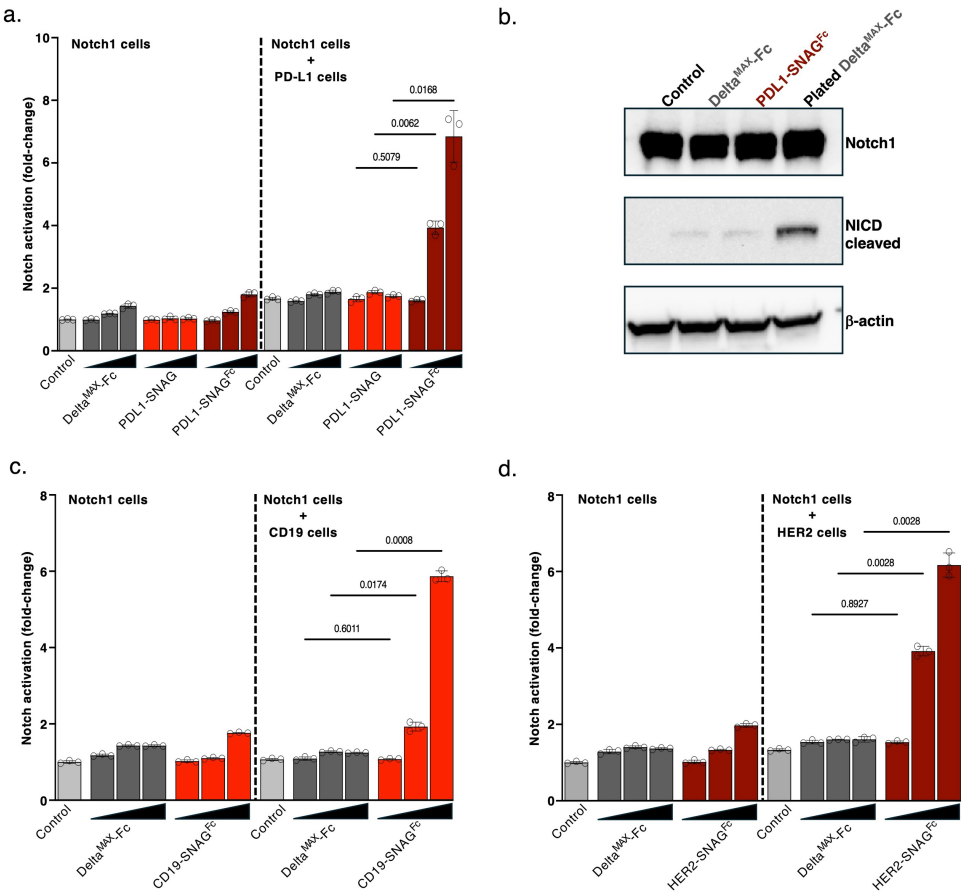

Figure. 4. SNAGs targeting tumor antigens activate Notch in mixed cell populations. (a) PDL1-SNAG-mediated activation of Notch1 was evaluated in a fluorescent reporter assay. Increasing concentrations (1 nM, 10 nM, or 100 nM) of Delta^{MAX}-Fc, PDL1-SNAG, or PDL1-SNAG^{Fc} were added to Notch1-Gal4 mCitrine reporter cells alone, or a 1:1 mixture of Notch1 reporter cells and MDA-MB-231 cells. (b) Activation of Notch1 in MDA-MB-231 cells, which express both PDL1 and Notch1, was assessed by Western Blot using an antibody against the activated NICD. (c, d). Notch1 activation by CD19-SNAGs and HER2-SNAGs, was evaluated using a fluorescent reporter assay. Increasing concentrations (1 nM, 10 nM, or 100 nM) of Delta^{MAX}-Fc or each SNAG^{Fc} were added to Notch1-Gal4 mCitrine reporter cells alone, or a 1:1 mixture of Notch1 reporter cells and CD19-overexpressing 3T3 cells (c) or HER2-expressing SK-BR-3 cells (d). For a, c, and d, a representative experiment from three biological replicates is shown. Mean fluorescence intensity (MFI) was normalized to the mean MFI of Notch1 reporter cells alone. Error bars represent the standard deviation of three technical replicates with the *P* value by Student's *t* test shown above each comparison.

309

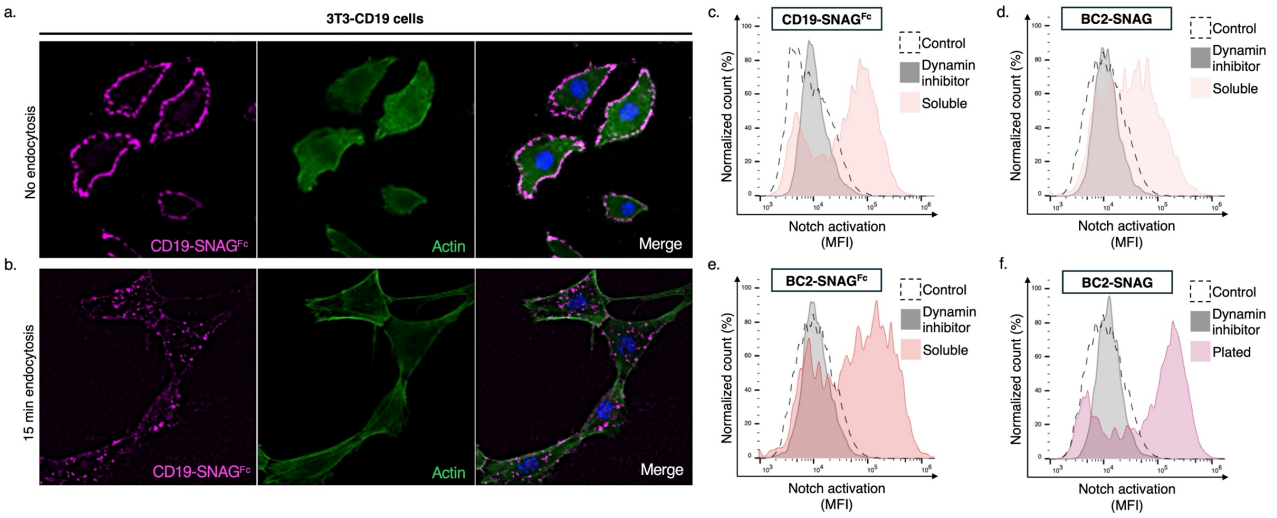

310
311

312 **Figure 5. SNAG-mediated Notch activation requires endocytosis.** (a) Representative
313 immunofluorescence images of fluorescently labeled CD19-SNAGs (magenta) used to stain the
314 surface of CD19 expressing 3T3 cells that were kept on ice. CD19-SNAGs visualized by Alexa
315 Fluor anti-Fc 647. To visualize the contours of the cells, the actin cytoskeleton was stained using
316 phalloidin-488 (green). Nuclei counterstained by Hoechst 33342 (blue). (b) Representative
317 immunofluorescence images of fluorescently labeled CD19-SNAGs used to stain the surface of
318 CD19 expressing 3T3 cells, followed by washing away unbound SNAGs and subjecting the cells
319 to a 15 min incubation in a 37 ºC incubator to resume cellular processes including endocytosis.
320 After 15 min the cells were fixed and stained in parallel with the no endocytosis samples. (d-e)
321 Flow cytometry histogram overlays depicting Notch1 reporter activity induced by soluble CD19-
322 SNAG^{Fc}, BC2-SNAG, or BC2-SNAG^{Fc} in the presence or absence of Dynasore. (c) Notch1
323 reporter cells were co-cultured with CD19-overexpressing 3T3 cells. In (d) and (e), Notch1
324 reporter cells were co-cultured with HEK293 cells expressing DLL4^{HL}. (f) Flow cytometry
325 histogram overlay depicting Notch1 reporter activity induced by immobilized BC2-SNAG in the
326 presence or absence of Dynasore. A representative histogram is shown for each experimental
327 condition from one of three biological replicates.

328
329

MATERIALS AND METHODS

Protein expression and purification

All SNAG sequences were cloned into a pAcGP67A vector for insect cell production containing an N-terminal gp67 signal peptide and C-terminal 8xHis-tag. Monomeric SNAGs were generated by fusing a truncated version of the Delta^{MAX} protein spanning from the N-terminus to EGF5 (N-EGF5) fused to a biomarker-targeting scFv or nanobody using a flexible $(GS)_5$ linker. Dimeric SNAG^{Fc} constructs were generated by fusing Delta^{MAX} (N-EGF5) and the biomarker targeting module to the N- and C-termini of a human IgG1 Fc domain, respectively. All SNAG^{Fc} constructs contained short GSG-linkers between the Fc sequence and Delta^{MAX} or the targeting module. Published sequences of atezolizumab, trastuzumab, and loncastuximab[49] were converted into a scFv format prior to being incorporated into SNAGs, and the sequence of the BC2-specific nanobody[32] was obtained from the Protein Data Bank (PDB ID 5VIN). Each scFv was generated by fusing the C-terminus of the variable heavy (V_H) domain to the N-terminus of the variable light (V_L) domain with a $(GGGGS)_3$ linker. Biotinylated Delta^{MAX}(N-EGF5) protein was generated through enzymatic modification of a C-terminal biotin acceptor peptide (BirA tag) as previously described[29]. The “headless” loss-of-function DLL4^{HL} mutant was generated by replacing the C2 and DSL domains of human DLL4 with the BC2-peptide sequence, which was connected to the N-terminus of EGF1 by a short GSG-linker. The DLL4^{HL} construct was cloned into a pLenti-IRES-Puro vector for mammalian expression.

All SNAG constructs in this study were expressed for by infecting *Trichoplusia ni* insect cell cultures (Expression Systems) at a density of 2×10^6 cells ml^{-1} with recombinant Baculovirus. Culture supernatants were harvested after 48h, and proteins were purified by nickel and size-exclusion chromatography. Biotinylated proteins were site-specifically modified using BirA ligase and excess biotin was removed by purifying the proteins on a size-exclusion column. Protein purity was assessed by SDS–PAGE using TGX 12% Precast gels (Bio-Rad). All proteins were flash-frozen in liquid nitrogen and stored at –80 °C following purification.

Cell culture and generation of cell lines

Mammalian cells were cultured at 37 °C, with a humidified atmosphere of 5% CO2, washed with Dulbecco’s PBS (DPBS, Corning), and detached with trypsin–EDTA 0.25% (Gibco) for subculturing or cell-based assays. Notch reporter cell lines CHO-K1 N1-Gal4 were a gift from Dr.

Michael Elowitz (California Institute of Technology)[30]. Briefly, transfections of HEK293T cells were carried out with packaging vectors VSV-G and d8.9 in the presence of polyethyleneimine at a ratio of 4:1 (DNA:polyethyleneimine). HER2+ SK-BR-3 cells, human CD19-overexpressing 3T3 cells, and PD-L1+ MDA-MB-231 cells were gifts from Drs. Brian Czerniecki, Fred Locke, and Eric Lau, respectively (Moffit Cancer Center). HEK293T, SK-BR-3, 3T3 mouse fibroblast, and MDA-MB-231 cells were cultured in high-glucose DMEM (Cytiva) supplemented with 10% FBS (peak serum) and 2% penicillin/streptomycin (Gibco). Puromycin 5 μg ml^{-1} was added to HEK293T cell cultures to maintain homogeneous populations of receptor-expressing cells. CHO-K1 N1-Gal4 cells were cultured in minimum essential medium Eagle-alpha modification (α-MEM, Cytiva) supplemented with 10% FBS (peak serum), 2% penicillin/streptomycin (Gibco), 400 μg ml–1 of zeocin (Alfa aesar) and 600 μg ml–1 of geneticin (Gibco). Expression of receptors on the cell surface was confirmed by flow cytometry (BD Accuri C6 plus) staining the cell lines with anti-hDLL4 PE, anti-hPDL1 FITC, anti-hHER2 (anti-IgG FITC), or anti-hCD19 FITC in DMEM supplemented with 10% FBS for 1 h at 4 °C.

Notch activation with Delta^{MAX} multimers

On day one, biotinylated Delta^{MAX}, Delta^{MAX} tetramers formed with streptavidin, or Delta^{MAX}-Fc were reconstituted in DPBS and adsorbed to tissue culture 96-well plates (Coastar) for 1 h at 37 °C. The wells were then washed three times with 200 µl of DPBS to remove unbound proteins. Next, CHO-K1 N1-Gal4 cells were detached with trypsin–EDTA 0.25% (Gibco) and manually counted. Appropriate dilutions were prepared in α-MEM media to ensure 30,000 CHO-K1 N1-Gal4 cells per well in a volume of 50 µL. Cells were transferred to the ligand-coated plates and cultured for 24 h at 37 °C in 5% CO2. On day two, CHO-K1 N1-Gal4 cells were washed with 200 μl DPBS, detached with 30 μL of trypsin–EDTA 0.25%, and quenched with 170 µL of α-MEM media. Finally, cells were resuspended, and the H2B-mCitrine signal was measured by flow cytometry (BD Accuri C6 plus). CHO-K1 N1-Gal4 cells alone were used as the control. The measurements represent the mean fluorescent intensity as fold-change of Notch activation ± s.d. of three technical replicates. Notch activation was normalized to wells containing CHO-K1 N1-Gal4 cells alone.

Notch activation with SNAGs in coculture of cells expressing the target tumor biomarker

On day one, cells expressing the target receptor of the SNAG (signal-sending cells) were detached with trypsin–EDTA, counted manually, and dilutions prepared such that 50 μL of DMEM containing 15,000 signal-sender cells were added to wells of a tissue culture 96-well plate. The next day, CHO-K1 N1-Gal4 reporter cells (signal-receiver cells) were detached with trypsin–EDTA, and 50 μl of α-MEM media containing 30,000 cells were added to the tissue culture 96-well plate containing the signal-sending cells after combining with the indicated Delta^{MAX} or SNAG protein. Wells without signal-sending cells were used to determine background activation of Notch by Delta^{MAX} and SNAGs. When testing inhibition of endocytosis, 80 μM of the Dynamin inhibitor I (Dynasore, Sigma) was added to the mixture of Notch reporter cells with protein and added to the tissue culture 96-well plate containing the signal-sending cells. Notch activation was measured as previously described.

Testing for Notch1 activation by the PDL1-SNAG^{Fc} in MDA-MB-231 cells. Delta^{MAX} (100 nM protein in 600 μL of DPBS) was non-specifically adsorbed to a single well of a 12-well plate for 1 hour at 37 ºC as a positive control for Notch1 activation. The positive control well and three additional wells were then seeded with 200 x 10^3 cells with MDA-MB-231 cells. The plate was centrifuged at 400 x *g* for 4 min to ensure cells were retained at the bottom of each well, and then the media of all wells was discarded. In the first uncoated well, 600 μL of DMEM was added as a negative control. The second well was filled with 600 μL of media containing 100 nM of Delta^{MAX}-Fc to monitor Notch1 activation by soluble ligand. The third was filled with 600 μL of media containing 100 nM PDL1-SNAG^{Fc}. The following day, the media was aspirated from all four wells, and the samples were resuspended in 60 μL of Laemli sample buffer with 5% β-mercaptoethanol to lyse cells, followed by boiling at 100 °C for 4 min. Lastly, the samples were analyzed by western blotting using equal protein amounts of cell lysates separated by SDS–PAGE (12% Mini-PROTEAN TGX Precast Protein Gels, Bio-Rad) and transferred to PVDF membranes using an iBlot2 Gel Transfer Device (Thermo Fisher Scientific). The membranes were blocked in 3% BSA + 0.1% TBS-Tween. Primary antibodies were anti-Notch1 (D1E11 rabbit mAb, Cell Signaling Technology, 1:1,000), anti-cleaved Notch1 (Val1744 rabbit mAb, Cell Signaling Technology, 1:1,000), and β-actin (rabbit polyclonal Ab, Cell Signaling Technology, 1:1,000). Secondary antibody anti-Rabbit IgG conjugated to HRP (Goat polyclonal Ab, Vector Laboratories, 1:8,000) was used for detection of proteins using SuperSignal West Pico PLUS Chemiluminescent

Substrate (Thermo Fisher Scientific). Images were acquired using a Chemidoc Imaging System and analyzed with Image-Lab v.6 software (Bio-Rad).

Immunofluorescent cell staining. For endocytosis assays, cells were grown on glass-like polymer bottoms in 24 well black frame plates (Cellvis). For visualization of CD19-SNAG^{Fc} protein binding, 500 nM protein was preincubated with anti-Fc 647 (Alexa Fluor) at 1:200 dilution for 1h on rotation in +4°C. The CD19-SNAG^{Fc}-647 solution was added to cells on ice that were further kept in +4°C for 1 h. For endocytosis, the incubation was followed by washing away non-bound CD19-SNAG^{Fc}-647 with PBS, and 37°C DMEM added to the cells followed by a 15 min incubation in a 37°C incubator. After incubation of CD19-SNAG^{Fc}-647 with or without endocytosis, the cells were fixed in 3% paraformaldehyde and permeabilized with 0.15% Triton X-100 in PBS for 10 min at RT. Nonspecific binding was blocked by incubation in 3% BSA in PBS with 0.05% Triton X-100 and 0.1M glycine for 60 min at RT. Cells were further stained for filamentous actin with Alexa 488 conjugated to phalloidin (Invitrogen) for 45 min to visualize contours of the individual cells. Hoechst 33342 (Invitrogen) was used to counterstain nuclei. Images were acquired using a Keyence BZ-X710 microscope using a Nikon Plan Apo 20x objective. The far-red channel (magenta) was processed with the de-haze function in the BZ-X710LE analyzer software. A minimum of 100 cells were imaged for each condition.

REFERENCES

1. Meloty-Kapella, L., Shergill, B., Kuon, J., Botvinick, E. & Weinmaster, G. Notch ligand endocytosis generates mechanical pulling force dependent on dynamin, epsins, and actin. *Dev. Cell* **22**, 1299–1312 (2012).
2. Wang, X. & Ha, T. Defining Single Molecular Forces Required to Activate Integrin and Notch Signaling. *Science* **340**, 991–994 (2013).
3. Gordon, W. R. *et al.* Mechanical Allostery: Evidence for a Force Requirement in the Proteolytic Activation of Notch. *Dev. Cell* **33**, 729–736 (2015).

4. Sprinzak, D. & Blacklow, S. C. Biophysics of Notch Signaling. *Annu Rev Biophys* **50**, 157–189 (2021).
5. Rebay, I. *et al.* Specific EGF repeats of Notch mediate interactions with Delta and Serrate: implications for Notch as a multifunctional receptor. *Cell* **67**, 687–699 (1991).
6. Luca, V. C. *et al.* Structural biology. Structural basis for Notch1 engagement of Delta-like 4. *Science* **347**, 847–853 (2015).
7. Luca, V. C. *et al.* Notch-Jagged complex structure implicates a catch bond in tuning ligand sensitivity. *Science* eaaf9739 (2017) doi:10.1126/science.aaf9739.
8. Gordon, W. R. *et al.* Structural basis for autoinhibition of Notch. *Nat. Struct. Mol. Biol.* **14**, 295–300 (2007).
9. De Strooper, B. *et al.* A presenilin-1-dependent gamma-secretase-like protease mediates release of Notch intracellular domain. *Nature* **398**, 518–522 (1999).
10. Brou, C. *et al.* A novel proteolytic cleavage involved in Notch signaling: the role of the disintegrin-metalloprotease TACE. *Mol. Cell* **5**, 207–216 (2000).
11. Schroeter, E. H., Kisslinger, J. A. & Kopan, R. Notch-1 signalling requires ligand-induced proteolytic release of intracellular domain. *Nature* **393**, 382–386 (1998).
12. Garg, V. *et al.* Mutations in NOTCH1 cause aortic valve disease. *Nature* **437**, 270–274 (2005).
13. Li, L. *et al.* Alagille syndrome is caused by mutations in human Jagged1, which encodes a ligand for Notch1. *Nat. Genet.* **16**, 243–251 (1997).
14. Joutel, A. *et al.* Notch3 mutations in CADASIL, a hereditary adult-onset condition causing stroke and dementia. *Nature* **383**, 707–710 (1996).
15. Bulman, M. P. *et al.* Mutations in the human delta homologue, DLL3, cause axial skeletal defects in spondylocostal dysostosis. *Nat Genet* **24**, 438–441 (2000).

16. Radtke, F. & Raj, K. The role of Notch in tumorigenesis: oncogene or tumour suppressor? *Nat Rev Cancer* **3**, 756–767 (2003).

17. Hori, K., Sen, A. & Artavanis-Tsakonas, S. Notch signaling at a glance. *Journal of Cell Science* **126**, 2135–2140 (2013).

18. Andersson, E. R. & Lendahl, U. Therapeutic modulation of Notch signalling--are we there yet? *Nat Rev Drug Discov* **13**, 357–378 (2014).

19. Brandstadter, J. D. & Maillard, I. Notch signalling in T cell homeostasis and differentiation. *Open Biol* **9**, 190187 (2019).

20. Schmitt, T. M. & Zúñiga-Pflücker, J. C. Induction of T Cell Development from Hematopoietic Progenitor Cells by Delta-like-1 In Vitro. *Immunity* **17**, 749–756 (2002).

21. Kelliher, M. A. & Roderick, J. E. NOTCH Signaling in T-Cell-Mediated Anti-Tumor Immunity and T-Cell-Based Immunotherapies. *Front Immunol* **9**, 1718 (2018).

22. Sierra, R. A. *et al.* Rescue of notch-1 signaling in antigen-specific CD8+ T cells overcomes tumor-induced T-cell suppression and enhances immunotherapy in cancer. *Cancer Immunol Res* **2**, 800–811 (2014).

23. Wilkens, A. B. *et al.* NOTCH1 signaling during CD4+ T-cell activation alters transcription factor networks and enhances antigen responsiveness. *Blood* **140**, 2261–2275 (2022).

24. Kondo, T. *et al.* Notch-mediated conversion of activated T cells into stem cell memory-like T cells for adoptive immunotherapy. *Nat Commun* **8**, 15338 (2017).

25. Varnum-Finney, B. *et al.* Immobilization of Notch ligand, Delta-1, is required for induction of notch signaling. *J. Cell. Sci.* **113 Pt 23**, 4313–4318 (2000).

26. Trotman-Grant, A. C. *et al.* DL4-µbeads induce T cell lineage differentiation from stem cells in a stromal cell-free system. *Nat Commun* **12**, 5023 (2021).

27. Li, K. *et al.* Modulation of Notch Signaling by Antibodies Specific for the Extracellular Negative Regulatory Region of NOTCH3. *J. Biol. Chem.* **283**, 8046–8054 (2008).

503 28. Tiyanont, K., Wales, T. E., Siebel, C. W., Engen, J. R. & Blacklow, S. C. Insights into Notch3
504 Activation and Inhibition Mediated by Antibodies Directed Against its Negative Regulatory
505 Region. *J Mol Biol* **425**, 3192–3204 (2013).
506 29. Gonzalez-Perez, D. *et al.* Affinity-matured DLL4 ligands as broad-spectrum modulators of
507 Notch signaling. *Nat Chem Biol* 1–9 (2022) doi:10.1038/s41589-022-01113-4.
508 30. Sprinzak, D. *et al.* Cis-interactions between Notch and Delta generate mutually exclusive
509 signalling states. *Nature* **465**, 86–90 (2010).
510 31. Cordle, J. *et al.* A conserved face of the Jagged/Serrate DSL domain is involved in Notch
511 trans-activation and cis-inhibition. *Nat Struct Mol Biol* **15**, 849–857 (2008).
512 32. Braun, M. B. *et al.* Peptides in headlock – a novel high-affinity and versatile peptide-binding
513 nanobody for proteomics and microscopy. *Sci Rep* **6**, (2016).
514 33. Powles, T. *et al.* MPDL3280A (anti-PD-L1) treatment leads to clinical activity in metastatic
515 bladder cancer. *Nature* **515**, 558–562 (2014).
516 34. Xiao, D. *et al.* Development of bifunctional anti-PD-L1 antibody MMAE conjugate with
517 cytotoxicity and immunostimulation. *Bioorganic Chemistry* **116**, 105366 (2021).
518 35. Zammarchi, F. *et al.* ADCT-402, a PBD dimer-containing antibody drug conjugate targeting
519 CD19-expressing malignancies. *Blood* **131**, 1094–1105 (2018).
520 36. Lewis Phillips, G. D. *et al.* Targeting HER2-positive breast cancer with trastuzumab-DM1, an
521 antibody-cytotoxic drug conjugate. *Cancer Res* **68**, 9280–9290 (2008).
522 37. Parks, A. L., Klueg, K. M., Stout, J. R. & Muskavitch, M. A. Ligand endocytosis drives
523 receptor dissociation and activation in the Notch pathway. *Development* **127**, 1373–1385
524 (2000).
525 38. Koo, B.-K. *et al.* An obligatory role of mind bomb-1 in notch signaling of mammalian
526 development. *PLoS One* **2**, e1221 (2007).

527 39. McMillan, B. J. *et al.* A tail of two sites: a bipartite mechanism for recognition of notch
528 ligands by mind bomb E3 ligases. *Mol Cell* **57**, 912–924 (2015).
529 40. Cao, R. *et al.* Structural Requirements for Activity of Mind bomb1 in Notch Signaling.
530 *bioRxiv* 2024.03.01.582834 (2024) doi:10.1101/2024.03.01.582834.
531 41. Kirchhausen, T., Macia, E. & Pelish, H. E. USE OF DYNASORE, THE SMALL MOLECULE
532 INHIBITOR OF DYNAMIN, IN THE REGULATION OF ENDOCYTOSIS. *Methods Enzymol*
533 **438**, 77–93 (2008).
534 42. Medina, E., Perez, D. H., Antfolk, D. & Luca, V. C. New tricks for an old pathway: emerging
535 Notch-based biotechnologies and therapeutics. *Trends Pharmacol Sci* S0165-
536 6147(23)00213–4 (2023) doi:10.1016/j.tips.2023.09.011.
537 43. Bonnici, L., Suleiman, S., Schembri-Wismayer, P. & Cassar, A. Targeting Signalling
538 Pathways in Chronic Wound Healing. *International Journal of Molecular Sciences* **25**, 50
539 (2024).
540 44. Mazor, Y. *et al.* Enhanced tumor-targeting selectivity by modulating bispecific antibody
541 binding affinity and format valence. *Sci Rep* **7**, 40098 (2017).
542 45. Haber, L. *et al.* Generation of T-cell-redirecting bispecific antibodies with differentiated
543 profiles of cytokine release and biodistribution by CD3 affinity tuning. *Sci Rep* **11**, 14397
544 (2021).
545 46. del Álamo, D., Rouault, H. & Schweisguth, F. Mechanism and Significance of cis-Inhibition
546 in Notch Signalling. *Current Biology* **21**, R40–R47 (2011).
547 47. Xu, X. *et al.* Insights into Autoregulation of Notch3 from Structural and Functional Studies of
548 Its Negative Regulatory Region. *Structure* **23**, 1227–1235 (2015).
549 48. Smyrlaki, I. *et al.* Soluble and multivalent Jag1 DNA origami nanopatterns activate Notch
550 without pulling force. *Nat Commun* **15**, 465 (2024).

551 49. Abanades, B. *et al.* The Patent and Literature Antibody Database (PLAbDab): an evolving
552 reference set of functionally diverse, literature-annotated antibody sequences and
553 structures. *Nucleic Acids Research* **52**, D545–D551 (2024).

554